PLANETARY SCIENCE

Detection of ammonia on Pluto's surface in a region of geologically recent tectonism

C. M. Dalle Ore[1,2]*, D. P. Cruikshank[2]*, S. Protopapa[3], F. Scipioni[1,2], W. B. McKinnon[4], J. C. Cook[5], W. M. Grundy[6], B. Schmitt[7], S. A. Stern[3], J. M. Moore[2], A. Verbiscer[8], A. H. Parker[3], K. N. Singer[3], O. M. Umurhan[1,2], H. A. Weaver[9], C. B. Olkin[3], L. A. Young[3], K. Ennico[2], New Horizons Surface Composition Science Theme Team†

We report the detection of ammonia (NH_3) on Pluto's surface in spectral images obtained with the New Horizons spacecraft that show absorption bands at 1.65 and 2.2 μm. The ammonia signature is spatially coincident with a region of past extensional tectonic activity (Virgil Fossae) where the presence of H_2O ice is prominent. Ammonia in liquid water profoundly depresses the freezing point of the mixture. Ammoniated ices are believed to be geologically short lived when irradiated with ultraviolet photons or charged particles. Thus, the presence of NH_3 on a planetary surface is indicative of a relatively recent deposition or possibly through exposure by some geological process. In the present case, the areal distribution is more suggestive of cryovolcanic emplacement, however, adding to the evidence for ongoing geological activity on Pluto and the possible presence of liquid water at depth today.

INTRODUCTION

Some small bodies in the solar system preserve a record of the events and chemistry of the solar nebula in which they formed and thereby carry chemical signatures of the molecular cloud from which the nebula condensed. Those bodies that have not been geologically and geochemically reprocessed carry the most pristine records. Ammonia is a potentially important source of nitrogen in the solar system and plays a pivotal role in planetary chemistry; until the work presented here, ammonia had not been detected spectroscopically on Pluto. The ammonia found in molecular clouds (*1*) and incorporated into condensing planetesimals, and comets (*2*), is especially important in the synthesis of organic materials found in certain meteorites (*3*, *4*) and is therefore a critical component in the chain of abiotic events, leading to planetary biochemical environments. In H_2O-rich bodies, NH_3 also has the effect of lowering the melting temperature, thereby helping to maintain liquid in their interiors (*5*). Although NH_3 is stable against evaporation for the age of the solar system on distant small bodies (*6*, *7*), it can be readily destroyed by ultraviolet (UV) radiation or ion bombardment as a free molecule or when frozen in ice. This process is enhanced when NH_3 occurs in H_2O ice (*8*). Therefore, NH_3 presence on a surface suggests a geologically relatively short lifetime and can be indicative of a young or renewed surface (*9*). However, its presence on the ancient surfaces of Pluto's small satellites indicates that ammonia may be able to survive for a long time in that environment, perhaps by being in a more durable chemical form such as a hydrate ($NH_3 \bullet nH_2O$) or as an ammoniated salt (*10*). In general, the form of the ammonia deduced from the spectral evidence available in current astronomical observations is ambiguous because absorption features in solid NH_3, hydrates, and ammoniated salts are weak combination bands with broad shapes and central wavelengths that overlap.

Pluto's surface was observed at high spatial resolution by the near-infrared spectral imager [Linear Etalon Imaging Spectral Array (LEISA), ~2700 m per pixel] and charge-coupled device camera [Multi-spectral Visible Imaging Camera (MVIC), ~650 m per pixel] system (*11*) on the New Horizons spacecraft during the flyby in 2015 (*12*–*14*). In the narrow geographic region of Pluto scanned at highest resolution, Cthulhu (some of the place and feature names on Pluto used in this paper are informal) is a central feature, with a dark red-brown color indicating a substantial non-ice composition rich in materials processed both in the atmosphere and on the surface and regarded as tholins (*13*). In the northern part of Cthulhu, two geographic features stand out: Elliot crater and the adjacent Virgil Fossae troughs, whose main component (hereafter Virgil Fossa) has a unique red color as seen in the color-enhanced MVIC image (Fig. 1B). A few small craters nearby share this distinctive coloration. The red-colored region in and around the fossa is spatially coincident with a prominent exposure of H_2O ice (as shown in Fig. 2B) that is seen in only a few other regions of Pluto's surface (*15*–*18*). In the enlarged view of the western portion of the fossa from the Pluto base map (Fig. 2A), shown also with the corresponding H_2O ice map derived from LEISA observations (Fig. 2B), muted topography (pit craters and fossa troughs) supports the contention that cryoclastic material was deposited from one or more erupting fountains. The apparent source of the fountains is within the main trough of the fossa, probably along the dip-slip fault defining the southern wall. The affected area is >5000 km^2, and other sources of fountaining and flow may occur in the same and adjacent areas that carry the H_2O and color signature.

Proceeding on the premise that Virgil Fossae and surroundings represent the site of cryovolcanic activity in the fractured crust of Pluto in a region of planet-wide stress induced by the formation of Sputnik Planitia (*19*, *20*) and subsequent events, we have investigated the composition of this region of interest (ROI) to understand its characteristics and the coincidence of the ammonia signature and red coloration with exposures of H_2O ice.

[1]SETI Institute, Mountain View CA, USA. [2]NASA Ames Research Center, Moffett Field CA, USA. [3]Southwest Research Institute, Boulder CO, USA. [4]Department of Earth and Planetary Sciences and the McDonnell Center for the Space Sciences, Washington University, St. Louis, MO, USA. [5]Pinhead Institute, Telluride CO, USA. [6]Lowell Observatory, Flagstaff AZ, USA. [7]Université Grenoble Alpes, CNRS, IPAG, F-38000 Grenoble, France. [8]Johns Hopkins University Applied Physics Laboratory, Laurel MD, USA. [9]University of Virginia, Charlottesville, VA, USA.
*Corresponding author. Email: cristina.m.dalleore@nasa.gov (C.M.D.O.); dale.p.cruikshank@nasa.gov (D.P.C.)
†The list of members of the New Horizons Surface Composition Science Theme Team can be found in the Supplementary Materials.

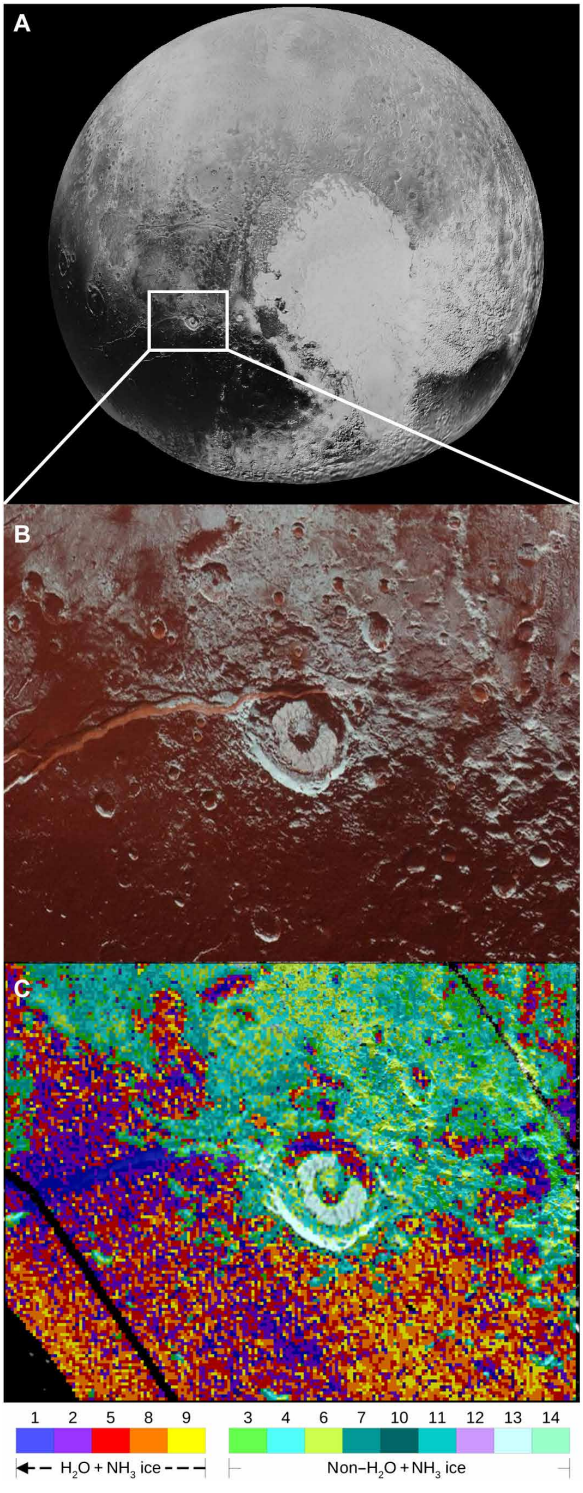

Fig. 1. Distribution of red-tinted H_2O ice exhibiting the spectral signature of NH_3 in Virgil Fossae and surrounding terrain. (**A**) Pluto's encounter hemisphere as seen by New Horizons during the 14 July 2015 flyby. (**B**) Selected ROI in the MVIC image illustrating the uniquely bright red coloring of Virgil Fossa. (**C**) Geographical distribution of the 14 clusters where clusters 1 (dark blue), 2 (purple), 5 (red), 8 (orange), and 9 (yellow) show the $H_2O + NH_3$–rich clusters in a gradation from maximum to minimum (indicated by the arrow direction). Image credit: NASA, Johns Hopkins University, Southwest Research Institute.

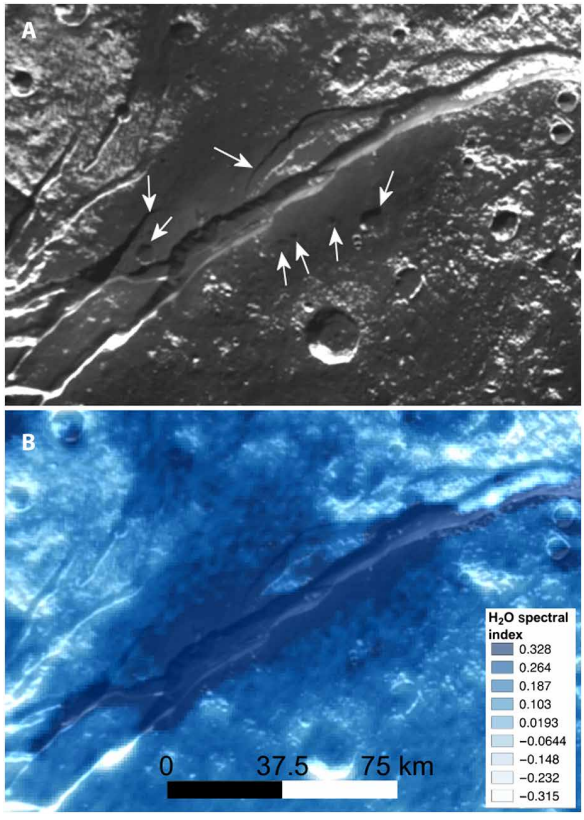

Fig. 2. Detail of the site of the putative cryovolcanic emission of NH_3-bearing H_2O in the main trough of Virgil Fossae. (**A**) Section of Virgil Fossae from the Pluto base map. Arrows point to topographic features that are muted in form by an apparent mantling by material ejected in a cryovolcanic event within the fossa main channel. (**B**) Same region shown with the H_2O ice distribution (*17*, *18*) in blue overlain on the base map: Darker shade of blue indicates greater concentration based on the strength of the ice absorption bands. Image credit: NASA, Johns Hopkins University, Southwest Research Institute.

RESULTS

Spectral analysis

We have studied the spectral signature of the ROI using a multivariate statistical analysis that classifies the spectra by their shape, in conjunction with radiative transfer modeling of the relevant spectra obtained from the classification process. We describe the approach in detail in the Materials and Methods.

The spectral averages obtained from the classification appear very similar to the eye, as shown in Fig. 3A, but map in a consistent way away from Virgil Fossa, as shown in Fig. 1C. To understand the differences that justify the classification, we adopted the spectrum of the class farthest away from the Virgil Fossa channel as our standard against which we compared, by means of a ratio, the other cluster averages. The ratios are shown in Fig. 3B and highlight spectral absorption bands characteristic of H_2O ice in a progression of increasing strength. A closer inspection revealed an anomalously deep 1.65-μm band and a depression in the shoulder of one of the H_2O bands at ~2.2 μm, typical of the spectral signature of NH_3. To confirm the detection, we computed a preliminary model of the spectrum of the ratio, a mixture of H_2O and tholin but no NH_3, shown in Fig. 4A_t and described in the Materials and Methods. The residuals of the observation ratioed to the model show a clear band at 2.2 μm (Fig. 4A_b).

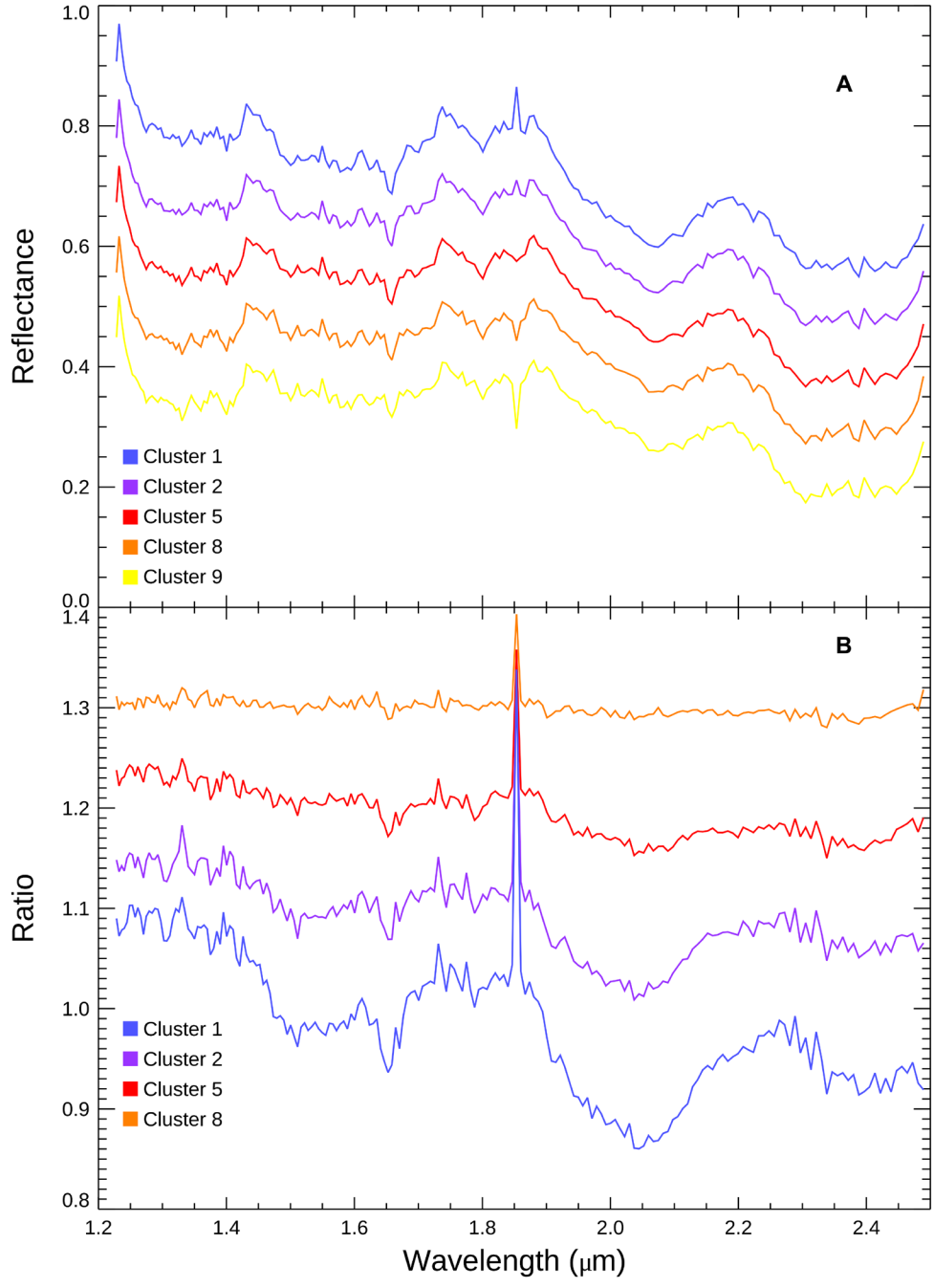

Fig. 3. Spectral signature of NH_3 in Virgil Fossae and surrounding terrain. (**A**) Averaged spectra for the CH_4-poor clusters 1, 2, 5, 8, and 9. Note that the raw spectra are similar. (**B**) Spectra of cluster 9 divided by clusters 1, 2, 5, and 8. The ratioed spectra reveal H_2O ice absorptions at 1.5, 1.65, and 2.0 μm and a depression at 2.2 μm characteristic of NH_3 products.

Comparison to satellites

A number of investigations of Pluto's largest moon Charon, as well as its smaller moons Nix and Hydra, have reported the presence of NH_3 or an ammoniated species revealed as a broad absorption band in the 2.2-μm spectral region (*21*–*25*, *10*). New Horizons observed Charon and the smaller satellites during the July 2015 flyby with the LEISA spectral imager at a spatial resolution of 4.87 km per pixel for Charon, 3.6 km per pixel for Nix, and 14.5 km per pixel for Hydra. NH_3 products were identified on Charon's surface in specific regions often corresponding to craters (*26*). In Fig. 4, we compare the NH_3 signature of Pluto (Fig. 4A), Charon (Fig. 4B), and Nix (Fig. 4C). The stronger absorption of Pluto's differential spectrum with respect to that of Charon is visible at 2.2 μm. The 2.2-μm absorption on Pluto and Nix is instead similar in depth and in the shape of the right wing of the band, as seen in the residual spectra, where the absorption on Pluto extends further toward shorter wavelengths. This may be due to the presence of other unidentified material(s) in the Virgil Fossa region. Overall, the consistent location and shape of the 2.2-μm

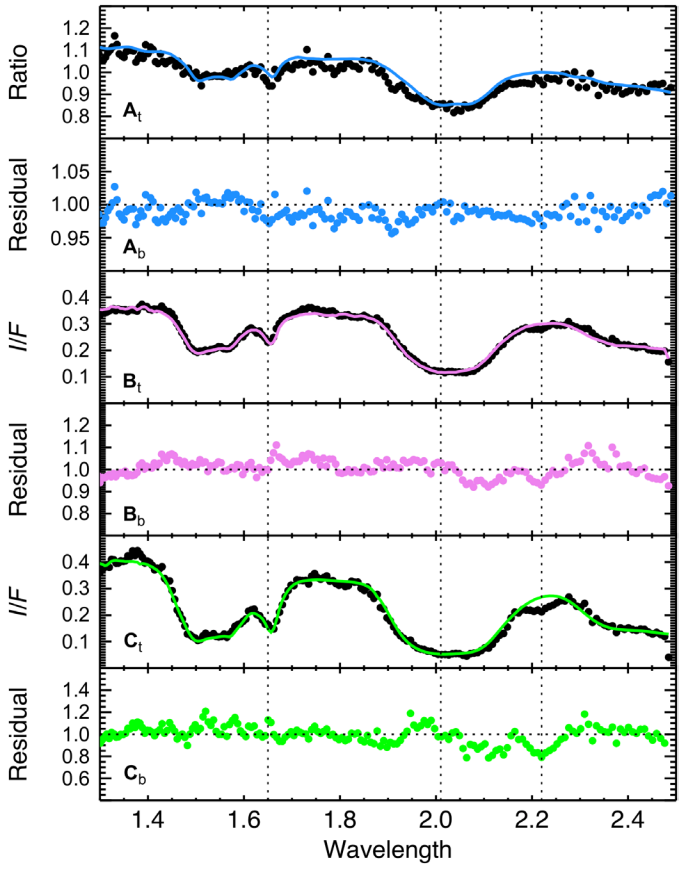

Fig. 4. Radiative transfer model fits to the derived spectra of NH_3-rich region of Virgil Fossae. Model fits (solid line, upper section of each panel) and residuals (lower section of each panel) obtained by dividing Pluto's ratio of cluster 9 to cluster 1 ($\mathbf{A}_t$ and $\mathbf{A}_b$), Charon's disk-averaged spectrum ($\mathbf{B}_t$ and $\mathbf{B}_b$), and Nix's disk-averaged spectrum ($\mathbf{C}_t$ and $\mathbf{C}_b$) by their corresponding best fits shown as a colored solid line. Models were calculated by means of either Hapke (*46*) or Shkuratov (*47*) approaches, including H_2O ice and a tholin, but not NH_3. Dashed vertical lines point to the wavelengths characteristic of the NH_3 spectrum. *I/F*, reflected intensity divided by incident solar flux.

band on Pluto's surface compared to the satellites demonstrate the strong presence of NH_3 and related species in some form on regions of Pluto's surface.

DISCUSSION

As noted, H_2O ice and the unique red coloration are spatially coherent, and the distribution of the H_2O-rich pixels, obtained with our multivariate analysis, shows areas where they clump in higher spatial concentration. These areas are located mainly along the Fossa, in a crater east of Elliot crater and possibly in a few patches north of the Fossa and Elliot crater. More isolated pixels are spread south and a few north of the Fossa.

Because H_2O ice is stable against evaporation at Pluto's temperatures, and in view of its sparse distribution across the surface, H_2O is regarded as the bedrock mostly covered from view by more volatile ices (N_2, CO, and CH_4) and non-ice components (tholins) and exposed only in some areas. Layers of more volatile ices alternate in cycles of sublimation and condensation with Pluto's seasons, contributing to the tenuous atmosphere of the planet (*27*) and accumulations of one or another of the ices in regions of different surface temperature [e.g., the concentration of N_2 ice in Sputnik Planitia (*17*)].

The coincidence of both H_2O and NH_3 absorption bands on localized regions of the surface may indicate exposure of NH_3 hydrate ice, which naturally forms from crystallization of H_2O-NH_3 fluids (*28*), or an ammoniated salt such as NH_4Cl or NH_4CO_3. Whereas in the hydrates, the central wavelength of the broad absorption band is 2.21 to 2.22 μm, in the salts, the broad band is generally centered between ~2.14 and 2.18 μm. Cook *et al.* (*10*) found that NH_4Cl gives a good fit to the shape and position of the ammonium band in both Nix and Hydra observed with New Horizons. Both of these small bodies also show strong bands of H_2O ice in the crystalline phase.

The ammonia or ammonium spectral signature is destroyed as the molecule is dissociated, and knowledge of its durability in Pluto's space environment is essential to an estimate of the age of the surface in which it is detected. The three principal sources of ammonia dissociation on the surface are UV photons, charged particles from the solar wind, and galactic cosmic rays (GCRs). UV photons come directly from the Sun and also from the interplanetary medium. The Lyman-α flux from the two sources combined is $\sim 7 \times 10^8$ photons cm^{-2} s^{-1} (*29*). The Lyman-α flux reaching the surface is modulated by the gaseous CH_4 content of the atmosphere. Models of the atmospheric content of CH_4 on annual and millennial time scales predict that the transparency of the atmosphere to Lyman-α flux varies from ~0.01 to 10%. Longer-wavelength UV radiation also contributes to the destruction of NH_3 (*9*). When NH_3 is dissociated, the fragments can combine quickly with other components in proximity. In a natural system, numerous other molecules and molecular fragments are expected, and in the presence of carbon species, a number of new molecules and radicals will form. Bernstein *et al.* (*30*), for example, found that in a mix of H_2O:CH_3OH:CO:NH_3 ices, about half of the N in NH_3 was incorporated into complex organic residues after exposures of $\sim 1 \times 10^{20}$ photons/cm^2. At times when Pluto's atmosphere is 10% transparent to Lyman-α photons, this flux corresponds to a time scale of $\sim 4 \times 10^5$ years, indicating a geologically short lifetime. At times of lower atmospheric transparency, the equivalent lifetime for the ammonia is $\sim 4 \times 10^8$ years.

Charged particles (e^-, H^+, and He^{2+}) from the solar wind interact with Pluto's tenuous atmosphere, and much of the flux is deflected around the planet (*31*). Some high-energy particles penetrate to the surface, although the flux is variable with atmospheric density, and the interaction with the surface materials is not well established. Both UV photons and solar wind charged particles deposit their energy in the uppermost few micrometers of Pluto's surface (*32*), and even for energetic particles, the secondary electrons initiate most of the chemical reactions (*33*). The spectral evidence reported here also represents the uppermost few micrometers of the surface and corresponds to the optical depth to which near-infrared reflectance spectroscopy is sensitive. Loeffler *et al.* (*9*) showed that the spectral signature of NH_3 in H_2O ice is quickly destroyed by 100-keV protons at 120 K but is much slower at lower temperatures more characteristic of Pluto's surface (~40 to 60 K). With specific reference to the NH_3 signature on Charon, Loeffler *et al.* (*9*) estimate that ~40% of the original ammonia has been destroyed over the 4.5–billion year age of the solar system.

GCRs penetrate several meters into a surface of pure H_2O ice or a mix of NH_3 in H_2O ice, depositing energy through secondary and higher-order interactions, ionizing molecules and atoms in their pathways. At the calculated rate of energy deposition for energies >10.5 eV,

slightly greater than the dissociation energy of the N—H bond in NH_3, the destruction of all NH_3 molecules in the upper 1-m layer of an ice composed of 30/70 NH_3:H_2O occurs in ~1.1×10^9 years. In an ice of this composition with no other impurities, dissociated NH_3 can readily recombine with an available electron from an H_2O molecule and indefinitely maintain a level of concentration. In a realistic ice, dissociated ammonia fragments will combine with other components, as noted above, and lose their spectral identity. Thus, in a real ice, 10^9 years can be taken as an upper limit to the longevity of the ammonia signature in the NH_3-H_2O ice surface in the Virgil Fossae region.

The ammonia spectral signature in ammoniated salts is expected to be more robust against destruction because ionic bonds are stronger than covalent bonds, but we are unaware of direct experimental evidence in support of this assertion. If the ammonia in Virgil Fossae is the signature of ammoniated salts, then the age of its deposition can be greater than if it arises instead from more fragile ammonia hydrates. In addition, if ammonia is replenished in the optical layer by diffusion of NH_3 upward through the H_2O ice [e.g., (*34*)], then the age of the initial deposition becomes indeterminate, but greater than if it comes from the hydrates.

While the age of the deposit of red-colored H_2O ice in the Virgil Fossae region is not well constrained by the durability of the NH_3 signature, it presents the appearance of a geologically recent cryovolcanic eruption or eruptions, emanating from a source of liquid water beneath Pluto's frozen surface ices (temperature, ~40 K), either now or in the past. In a concentration of ~33% NH_3 in liquid H_2O, the freezing point is depressed to 176 K. Presumably, such a mixture could remain as a fluid in the interior of Pluto, where the temperature is naturally higher than the surface because of the decay or radioactive elements in the rocky material comprising the majority of Pluto's mass (*35*). The liquid H_2O–NH_3 mixture could be part of a subsurface ocean (*20*) or a more localized crustal reservoir. Cracks or conduits in the icy crust could be routes of egress for the liquid H_2O–NH_3 that, upon reaching the vacuum and cold at the surface, both freezes and boils, forming fountains that shower the Fossa surroundings with icy particles.

The blue pixels in Fig. 1C, markers of areas of H_2O enriched with NH_3, are distributed south for more than 150 km and partly north of Virgil Fossa. They are concentrated as well as in sections of the Fossa itself, a channel through which liquid H_2O–NH_3, colored with the unique red chromophore, may have flowed from one or more vents before freezing in place. Outside the Fossa, the pixel distribution is suggestive of ejected dissemination of H_2O-NH_3 ice particles. The deeper H_2O bands could be due to differences in grain size where the larger grains might have been deposited closer to the eruption source or sources.

The ice in and around Virgil Fossa, which consists of H_2O contaminated with NH_3, has a unique red coloration, as seen in Fig. 1B. Non-ice surface materials having pronounced yellow-to-red coloration are thought to be products of energetic processing of CH_4 (or other carbon-bearing molecules) and N_2 (*13*) and are chemically similar to a strongly colored refractory organic solid [Pluto ice tholin (PIT)] produced in the laboratory by UV photolysis and charged-particle radiolysis of a mixture of CH_4 and N_2 ices (*36*, *37*). Energetic processing of the same molecular mixture in the gas phase also produces colored organic tholins (*38*), and similar chemistry enhanced by the presence of NH_3 may have occurred in subsurface liquid reservoirs on Pluto, if dissolved H_2CO was also present (*39*).

The Virgil Fossae complex is part of a tectonic pattern radiating away from Sputnik Planitia and the basin in which it lies (*14*). The ejection of fluid onto the surface through faults or cracks could be propelled by fluid pressure due to ocean or crustal reservoir freezing (*40*) and or by gas pressure due to exsolution in a cryovolcanic event, perhaps of the type described by Neveu *et al.* (*41*). Both the pattern and the relative freshness of the Virgil Fossa scarp are indicative of geologically relative youth or renewal of faults driven by basin-related stresses (*19*, *20*). Therefore, if cryovolcanism is involved in the creation of the ammonia-rich spectral signature described here, then it is further suggestive of both ongoing tectonism and escape of ammonia-bearing aqueous fluids presumably derived from an internal ocean or from a crustal reservoir ultimately sourced from the ocean.

MATERIALS AND METHODS

Multivariate analysis

To isolate the spectral signature of Virgil Fossa in the LEISA data, we used an unsupervised statistical clustering tool, i.e., a *k*-means classification tool made unsupervised by means of the Calinski-Harabasz (C-H) criterion (*42*). The clustering algorithm was applied to the spectral region between ~1.75 and ~2.22 μm. The C-H criterion selected three as the ideal number of clusters to represent the main variations in the area: no data, CH_4-rich, and CH_4-poor. However, we chose 14 classes of differing spectra (or clusters) in the adopted ROI to highlight subtle differences that go beyond the abundance of CH_4 ice. Of these classes, clusters 10 and 12 were too noisy to be considered, and another seven were dominated by absorption bands of CH_4 ice and mostly located in the northeast half of the region (colored teal in Fig. 1C). The remaining five classes were spread over the southwest part of the ROI, showing a spectral signature that could not be readily attributed either to an ice or to a refractory material. Figure 1C shows the distribution of the 14 clusters.

We focused our analysis on clusters 1, 2, 5, 8, and 9 whose spectral averages, offset for clarity, are shown in Fig. 3A. All clusters have a SD of $0.08 \leq \sigma \leq 0.10$ corresponding to the spectral variation of the spectra in the region adopted by the clustering. The cluster population varies from ~1500 to ~4000 pixels but does not correlate with the SD, confirming the fact that the SD is not a statistical measurement. One of them, cluster 1, included a strong concentration of pixels on and around Virgil Fossa (shown in dark blue in Fig. 1C). Although the spectral signature of this region is similar to those of the other four CH_4-poor classes (Fig. 3A), further analysis revealed important variations. To distinguish subtle differences between the average spectrum of Virgil Fossa (cluster 1) and spectra of its surroundings, we compared the spectral signatures by taking the ratio of the spectrum of cluster 9 by that of every other cluster average. Cluster 9 is the class that is geographically most distant from the Fossa and is believed to be the most H_2O-ice poor on the basis of H_2O distribution maps (Fig. 2B) (*18*). The resulting spectra (Fig. 3B) display evident H_2O ice signatures, particularly for the cluster 1 pixel average. In (Fig. 3B), the spectrum of cluster 9 is not shown again as it is adopted as the standard for comparing the spectra. We note that the trace showing the differential of cluster 8, with very shallow bands, is highlighting pixels that are spectrally very similar to those in cluster 9. Similarly, with the other class averages, the main difference highlighted in the traces is a progression in the depth of H_2O ice bands, culminating with the most H_2O-rich cluster average, cluster 1, geographically coincident with the main trough of Virgil Fossa.

Upon closer inspection of the differential spectra, the varying depth of the 1.65-μm H_2O ice band becomes evident. The depth of this band exceeds that of the 1.5-μm band for all classes, a behavior that is anomalous for pure H_2O ice. The spectra are also characterized by a depression of varying strength in the spectral region between 2.1 and 2.25 μm. Bands at these wavelengths are characteristic of NH_3 and its stoichiometric hydrates (*43*, *44*) as well as ammoniated salts. NH_3 ice has also an absorption band at ~2.0 μm that blends in with the strong H_2O band.

Geographical mapping

The spatial distribution of the pixels showing a contribution of NH_3 in H_2O according to the differential analysis described before is presented in Fig. 1C. It is overlain on a base map obtained from the corresponding LOng Range Reconnaissance Imager (LORRI) observations obtained during the flyby. Figure 1B shows the MVIC map for comparison. The strongest H_2O and NH_3 signature (blue pixels) are found in and near Virgil Fossa, with a few spread out in the neighboring areas, while regions with the shallowest H_2O and NH_3 bands (yellow pixels) are located away from Virgil Fossa. The remaining clusters are spread between these two extremes in a geographically homogeneous distribution. The different depths of the H_2O bands could be due either to variations in concentration or to the near-infrared path length in the ice. While more precise modeling will be needed to determine which of the two possibilities is correct, for the purpose of this paper, we identified all pixels in the clusters adopted for this study as H_2O-rich.

Modeling

To highlight the presence of NH_3 ice on Pluto, we calculated a rough model of the differential spectrum of cluster 1 shown in Fig. 3B and corresponding to the blue pixels in Fig. 1C. We used the following three components: H_2O ice, amorphous carbon (AC), and a refractory organic solid made by electron radiolysis of an ice mixture of N_2, CH_4, and CO (*37*), denoted as PIT, mixed intimately using the Shkuratov computational formulation (*45*). For the H_2O ice component, we used the optical constants in (*45*) and a grain size of 3 μm, contributing 83.5% to the mixture. The low-reflectance components, AC in 20-μm grains and PIT in grains of 15 μm, contributed at concentrations of 1.5 and 15%, respectively. PIT was produced in the laboratory by Materese *et al.* (*37*), and its optical constants were extracted from the reflectance spectrum. We note that the adopted grain size of the H_2O ice is very small and marginally acceptable in terms of the geometrical optics assumptions in the Shkuratov formulation. However, the purpose of the model is purely to highlight the presence of NH_3, and therefore, the relative abundances and grain sizes of the components included in the model should not be used in a quantitative way. We compared the model to the observations by calculating the residuals, shown in Fig. 4A_b along with corresponding spectra, models, and residuals of Charon and the smaller satellite Nix. Pluto's residual spectrum, obtained by dividing the observations by the model, shows a clear dip at both 1.65 and 2.2 μm. The 2.2-μm depression is wider than expected from contributions of pure NH_3 and NH_3 in H_2O (hydrates) and might include signatures of other compounds presently unidentified.

The 1.5- and 2.0-μm bands characteristic of a NH_3 signature are somewhat inconsistent. The NH_3 2.0-μm band is blended with the H_2O band, which is a much stronger feature in the H_2O than in the NH_3 spectrum. For this reason, it is difficult to disentangle the two contributions, even with a modeling approach. In our model (Fig. 4A_t), the residual spectrum shows a value close to 1 at 2.0 μm, indicative of a good fit to the depth of the band. The model is imperfect, however, leaving small discrepancies in band strength and continuum levels that might indicate the presence of another component aside from NH_3, presently unidentified. For example, the 1.65-μm band is too strong in the data when compared to a pure crystalline H_2O ice spectrum. Methane has a band close to this wavelength, but the lack of other stronger CH_4 bands in our data excludes this possibility.

Modeling the spectra of the satellites

Radiative transfer models based on Hapke or Shkuratov approaches have been applied to Charon (*26*) and Pluto's small satellites Nix and Hydra (*10*). Hapke as well as Shkuratov theory (*46*, *47*) rely on knowing the optical constants of each material included in the model. However, optical constants for ammonia hydrates are poorly known for several reasons, including the coarse wavelength sampling, the lack of data in the relevant wavelength range, and also the detailed structure (stoichiometry) of the material. Optical constants for ammoniated salts have not, to our knowledge, been measured. To model these spectra, the data were given lower statistical weight over the wavelength range of 2.18 to 2.24 μm, and the models consist of a mixture of amorphous and crystalline H_2O ice and PIT. The difference between the model and the observations highlighted the large absorption feature with a minimum at 2.21 μm, consistent with ammonia hydrates and ammoniated salts (e.g., NH_4Cl), all of which show the ammonia band at a slightly longer wavelength than pure NH_3.

SUPPLEMENTARY MATERIALS

Supplementary material for this article is available at http://advances.sciencemag.org/cgi/content/full/5/5/eaav5731/DC1

List of members of the New Horizons Surface Composition Science Theme Team.

REFERENCES AND NOTES

1. K. I. Öberg, A. C. A. Boogert, K. M. Pontoppidan, The *Spitzer* ice legacy: Ice evolution from cores to protostars. *Astrophys. J.* **740**, 109 (2011).
2. M. J. Mumma, S. B. Charnley, The chemical composition of comets—Emerging taxonomies and natal heritage. *Annu. Rev. Astron. Astrophys.* **49**, 471–524 (2011).
3. C. M. O'D. Alexander, L. R. Nittler, J. Davidson, F. J. Ciesla, Measuring the level of interstellar inheritance in the solar protoplanetary disk. *Meteorit. Planet. Sci.* **52**, 1797–1821 (2017).
4. S. Pizzarello, L. B. Williams, Ammonia in the early solar system: An account from carbonaceous meteorites. *Astrophys. J.* **749**, 161 (2012).
5. M. Neveu, S. J. Desch, J. C. Castillo-Rogez, Aqueous geochemistry in icy world interiors: Equilibrium fluid, rock, and gas compositions, and fate of antifreezes and radionuclides. *Geochim. Cosmochim. Acta* **212**, 324–371 (2017).
6. K. Watson, B. C. Murray, H. Brown, The stability of volatiles in the solar system. *Icarus* **1**, 317–327 (1963).
7. L. A. Lebofsky, Stability of frosts in the solar system. *Icarus* **25**, 205–217 (1975).
8. M. H. Moore, R. F. Ferrante, R. L. Hudson, J. N. Stone, Ammonia–water ice laboratory studies relevant to outer solar system surfaces. *Icarus* **190**, 260–273 (2007).
9. M. J. Loeffler, U. Raut, R. A. Baragiola, Radiation chemistry in ammonia-water ices. *J. Chem. Phys.* **132**, 054508 (2010).
10. J. C. Cook, C. M. Dalle Ore, S. Protopapa, R. P. Binzel, R. Cartwright, D. P. Cruikshank, A. Earle, W. M. Grundy, K. Ennico, C. Howett, D. E. Jennings, A. W. Lunsford, C. B. Olkin, A. H. Parker, S. Philippe, D. Reuter, B. Schmitt, J. A. Stansberry, S. Alan Stern, A. Verbiscer, H. A. Weaver, L. A. Young, Composition of Pluto's small satellites: Analysis of *New Horizons* spectral images. *Icarus* **315**, 30–45 (2018).
11. D. C. Reuter, S. A. Stern, J. Scherrer, D. E. Jennings, J. W. Baer, J. Hanley, L. Hardaway, A. Lunsford, S. McMuldroch, J. Moore, C. Olkin, R. Parizek, H. Reitsma, D. Sabatke, J. Spencer, J. Stone, H. Throop, J. van Cleve, G. E. Weigle, L. A. Young, Ralph: A visible/infrared imager for the New Horizons Pluto/Kuiper Belt mission. *Space Sci. Rev.* **140**, 129–154 (2008).
12. S. A. Stern, F. Bagenal, K. Ennico, G. R. Gladstone, W. M. Grundy, W. B. McKinnon, J. M. Moore, C. B. Olkin, J. R. Spencer, H. A. Weaver, L. A. Young, T. Andert, J. Andrews,

M. Banks, B. Bauer, J. Bauman, O. S. Barnouin, P. Bedini, K. Beisser, R. A. Beyer, S. Bhaskaran, R. P. Binzel, E. Birath, M. Bird, D. J. Bogan, A. Bowman, V. J. Bray, M. Brozovic, C. Bryan, M. R. Buckley, M. W. Buie, B. J. Buratti, S. S. Bushman, A. Calloway, B. Carcich, A. F. Cheng, S. Conard, C. A. Conrad, J. C. Cook, D. P. Cruikshank, O. S. Custodio, C. M. Dalle Ore, C. Deboy, Z. J. B. Dischner, P. Dumont, A. M. Earle, H. A. Elliott, J. Ercol, C. M. Ernst, T. Finley, S. H. Flanigan, G. Fountain, M. J. Freeze, T. Greathouse, J. L. Green, Y. Guo, M. Hahn, D. P. Hamilton, S. A. Hamilton, J. Hanley, A. Harch, H. M. Hart, C. B. Hersman, A. Hill, M. E. Hill, D. P. Hinson, M. E. Holdridge, M. Horanyi, A. D. Howard, C. J. A. Howett, C. Jackman, R. A. Jacobson, D. E. Jennings, J. A. Kammer, H. K. Kang, D. E. Kaufmann, P. Kollmann, S. M. Krimigis, D. Kusnierkiewicz, T. R. Lauer, J. E. Lee, K. L. Lindstrom, I. R. Linscott, C. M. Lisse, A. W. Lunsford, V. A. Mallder, N. Martin, D. J. McComas, R. L. McNutt Jr., D. Mehoke, T. Mehoke, E. D. Melin, M. Mutchler, D. Nelson, F. Nimmo, J. I. Nunez, A. Ocampo, W. M. Owen, M. Paetzold, B. Page, A. H. Parker, J. W. Parker, F. Pelletier, J. Peterson, N. Pinkine, M. Piquette, S. B. Porter, S. Protopapa, J. Redfern, H. J. Reitsema, D. C. Reuter, J. H. Roberts, S. J. Robbins, G. Rogers, D. Rose, K. Runyon, K. D. Retherford, M. G. Ryschkewitsch, P. Schenk, E. Schindhelm, B. Sepan, M. R. Showalter, K. N. Singer, M. Soluri, D. Stanbridge, A. J. Steffl, D. F. Strobel, T. Stryk, M. E. Summers, J. R. Szalay Jr., M. Tapley, A. Taylor, H. Taylor, H. B. Throop, C. C. C. Tsang, G. L. Tyler, O. M. Umurhan, A. J. Verbiscer, M. H. Versteeg, M. Vincent, R. Webbert, S. Weidner, G. E. Weigle, O. L. White, K. Whittenburg, B. G. Williams, K. Williams, S. Williams, W. W. Woods, A. M. Zangari, E. Zirnstein, The Pluto system: Initial results from its exploration by New Horizons. *Science* **350**, aad1815 (2015).

13. W. M. Grundy, R. P. Binzel, B. J. Buratti, J. C. Cook, D. P. Cruikshank, C. M. Dalle Ore, A. M. Earle, K. Ennico, C. J. A. Howett, A. W. Lunsford, C. B. Olkin, A. H. Parker, S. Philippe, S. Protopapa, E. Quirico, D. C. Reuter, B. Schmitt, K. N. Singer, A. J. Verbiscer, R. A. Beyer, M. W. Buie, A. F. Cheng, D. E. Jennings, I. R. Linscott, J. W. Parker, P. M. Schenk, J. R. Spencer, J. A. Stansberry, S. A. Stern, H. B. Throop, C. C. C. Tsang, H. A. Weaver, G. E. Weigle II, L. A. Young; New Horizons Science Team, Surface compositions across Pluto and Charon. *Science* **351**, aad9189 (2016).
14. J. M. Moore, W. B. McKinnon, J. R. Spencer, A. D. Howard, P. M. Schenk, R. A. Beyer, F. Nimmo, K. N. Singer, O. M. Umurhan, O. L. White, S. A. Stern, K. Ennico, C. B. Olkin, H. A. Weaver, L. A. Young, R. P. Binzel, M. W. Buie, B. J. Buratti, A. F. Cheng, D. P. Cruikshank, W. M. Grundy, I. R. Linscott, H. J. Reitsema, D. C. Reuter, M. R. Showalter, V. J. Bray, C. L. Chavez, C. J. A. Howett, T. R. Lauer, C. M. Lisse, A. H. Parker, S. B. Porter, S. J. Robbins, K. Runyon, T. Stryk, H. B. Throop, C. C. C. Tsang, A. J. Verbiscer, A. M. Zangari, A. L. Chaikin, D. E. Wilhelms; New Horizons Science Team, The geology of Pluto and Charon through the eyes of New Horizons. *Science* **351**, 1284–1293 (2016).
15. C. B. Olkin, J. R. Spencer, W. M. Grundy, A. H. Parker, R. A. Beyer, P. M. Schenk, C. J. A. Howett, S. A. Stern, D. C. Reuter, H. A. Weaver, L. A. Young, K. Ennico, R. P. Binzel, M. W. Buie, J. C. Cook, D. P. Cruikshank, C. M. Dalle Ore, A. M. Earle, D. E. Jennings, K. N. Singer, I. E. Linscott, A. W. Lunsford, S. Protopapa, B. Schmitt, E. Weigle; New Horizons Science Team, The global color of Pluto from New Horizons. *Astron. J.* **154**, 258 (2017).
16. J. C. Cook, D. P. Cruikshank, C. M. Dalle Ore, K. Ennico, W. M. Grundy, C. B. Olkin, S. Protopapa, S. A. Stern, H. A. Weaver, L. A. Young; New Horizons surface composition theme team, The identification and distribution of Pluto's non-volatile inventory, in *47th Lunar Planetary Science Conference*, The Woodlands, Texas, 21 to 26 March 2016.
17. S. Protopapa, W. M. Grundy, D. C. Reuter, D. P. Hamilton, C. M. Dalle Ore, J. C. Cook, D. P. Cruikshank, B. Schmitt, S. Philippe, E. Quirico, R. P. Binzel, A. M. Earle, K. Ennico, C. J. A. Howett, A. W. Lunsford, C. B. Olkin, A. Parker, K. N. Singer, S. A. Stern, A. J. Verbiscer, H. A. Weaver, L. A. Young, Pluto's global surface composition through pixel-by-pixel Hapke modeling of New Horizons Ralph/LEISA data. *Icarus* **287**, 218–228 (2017).
18. B. Schmitt, S. Philippe, W. M. Grundy, D. C. Reuter, R. Cote, E. Quirico, S. Protopapa, L. A. Young, R. P. Binzel, J. C. Cook, D. P. Cruikshank, C. M. Dalle Ore, A. M. Earle, K. Ennico, C. J. A. Howett, D. E. Jennings, I. R. Linscott, A. W. Lunsford, C. B. Olkin, A. H. Parker, K. N. Singer, J. R. Spencer, J. Stansberry, S. A. Stern, C. C. C. Tsang, A. J. Verbiscer, H. A. Weaver; New Horizons Science Team, Physical state and distribution of materials at the surface of Pluto from New Horizons LEISA imaging spectrometer. *Icarus* **287**, 229–260 (2017).
19. J. T. Keane, I. Matsuyama, S. Kamata, J. K. Steckloff, Reorientation and faulting of Pluto due to volatile loading within Sputnik Planitia. *Nature* **540**, 90–93 (2016).
20. F. Nimmo, D. P. Hamilton, W. B. McKinnon, P. M. Schenk, R. P. Binzel, C. J. Bierson, R. A. Beyer, J. M. Moore, S. A. Stern, H. A. Weaver, C. B. Olkin, L. A. Young, K. E. Smith; New Horizons Geology, Geophysics &Imaging Theme Team, Reorientation of Sputnik Planitia implies a subsurface ocean on Pluto. *Nature* **540**, 94–96 (2016).
21. M. W. Buie, W. M. Grundy, The Distribution and physical state of H_2O on Charon. *Icarus* **148**, 324–339 (2000).
22. M. E. Brown, W. M. Calvin, Evidence for crystalline water and ammonia ices on Pluto's satellite Charon. *Science* **287**, 107–109 (2000).
23. C. Dumas, R. J. Terrile, R. H. Brown, G. Schneider, B. A. Smith, *Hubble Space Telescope* NICMOS spectroscopy of Charon's leading and trailing hemispheres. *Astron. J.* **121**, 1163–1170 (2001).
24. J. C. Cook, S. J. Desch, T. L. Roush, C. A. Trujillo, T. R. Geballe, Near-infrared spectroscopy of Charon: Possible evidence for cryovolcanism on Kuiper Belt objects. *Astrophys. J.* **663**, 1406–1419 (2007).
25. A. J. Verbiscer, D. E. Peterson, M. F. Skrutskie, M. Cushing, M. J. Nelson, J. D. Smith, J. C. Wilson, Simultaneous spatially-resolved near-infrared spectra of Pluto and Charon, in 38th *Lunar Planetary Science Conference XXXVIII*, League City, Texas 12 to 16 March 2007.
26. C. M. Dalle Ore, S. Protopapa, J. C. Cook, W. M. Grundy, D. P. Cruikshank, A. J. Verbiscer, K. Ennico, C. B. Olkin, S. A. Stern, H. A. Weaver, L. A. Young; New Horizons Science Team, Ices on Charon: Distribution of H_2O and NH_3 from New Horizons LEISA observations. *Icarus* **300**, 21–32 (2017).
27. G. R. Gladstone, S. A. Stern, K. Ennico, H. A. Weaver, L. A. Young, M. E. Summers, D. F. Strobel, D. P. Hinson, J. A. Kammer, A. H. Parker, A. J. Steffl, I. R. Linscott, J. W. Parker, A. F. Cheng, D. C. Slater, M. H. Versteeg, T. K. Greathouse, K. D. Retherford, H. Throop, N. J. Cunningham, W. W. Woods, K. N. Singer, C. C. C. Tsang, E. Schindhelm, C. M. Lisse, M. L. Wong, Y. L. Yung, X. Zhu, W. Curdt, P. Lavvas, E. F. Young, G. L. Tyler; New Horizons Science Team, The atmosphere of Pluto as observed by New Horizons. *Science* **351**, aad8866 (2016).
28. N. Uras, J. P. Devlin, Rate study of ice particle conversion to ammonia hemihydrate: Hydrate crust nucleation and NH_3 diffusion. *J. Phys. Chem. A* **104**, 5770–5777 (2000).
29. G. R. Gladstone, W. R. Pryor, S. A. Stern, K. Ennico, C. B. Olkin, J. R. Spencer, H. A. Weaver, L. A. Young, F. Bagena, A. F. Chen, N. J. Cunningham, H. A. Elliott, T. K. Greathouse, D. P. Hinson, J. A. Kammer, I. R. Linscott, J. W. Parker, K. D. Retherford, A. J. Steff, D. F. Strobel, M. E. Summers, H. Throop, M. H. Versteeg, M. W. Davis, The Lyman; α sky background as observed by New Horizons. *Geophys. Res. Lett.* 45, 8022–8028 2018 10.1029/2018GL078808.
30. M. P. Bernstein, S. A. Sandford, L. J. Allamandola, H, C, N, and O isotopic substitution studies of the 2165 wavenumber (4.62 micron) "XCN" Feature produced by ultraviolet photolysis of mixed molecular ices. *Astrophys. J.* **542**, 894–897 (2000).
31. D. J. McComas, H. A. Elliott, S. Weidner, P. Valek, E. J. Zirnstein, F. Bagenal, P. A. Delamere, R. W. Ebert, H. O. Funsten, M. Horanyi, R. L. McNutt, C. Moser, N. A. Schwadron, D. F. Strobel, L. A. Young, K. Ennico, C. B. Olkin, S. A. Stern, H. A. Weaver, Pluto's interaction with the solar wind. *J. Geophys. Res. Space Phys.* **121**, 4232–4246 (2016).
32. C. J. Bennett, C. Pirim, T. M. Orlando, Space-weathering of solar system bodies: A laboratory perspective. *Chem. Rev.* **113**, 9086–9150 (2013).
33. R. L. Hudson, M. E. Palumbo, G. Strazzulla, M. H. Moore, J. F. Cooper, S. J. Sturner, Laboratory studies of the chemistry of transneptunian object surface materials, in *The Solar System Beyond Neptune*, M. A. Barucci, H. Boehnhardt, D. P. Cruikshank, A. Morbidelli, Eds. (University of Arizona Press, 2009), pp. 507–523.
34. B. J. Holler, L. A. Young, M. W. Buie, W. M. Grundy, J. E. Lyke, E. F. Young, H. G. Roe, Measuring temperature and ammonia hydrate ice on Charon in 2015 from Keck/OSIRIS spectra. *Icarus* **284**, 394–406 (2017).
35. W. B. McKinnon, S. A. Stern, H. A. Weaver, F. Nimmo, C. J. Bierson, J. C. Cook, W. M. Grundy, D. P. Cruikshank, A. H. Parker, J. M. Moore, J. R. Spencer, L. A. Young, C. B. Olkin, K. E. Smith; New Horizons Geology, Geophysics & Imaging and Composition Theme Teams, Origin of the Pluto-Charon system: Constraints from the New Horizons flyby. *Icarus* **287**, 2–11 (2017).
36. C. K. Materese, D. P. Cruikshank, S. A. Sandford, H. Imanaka, M. Nuevo, D. White, Ice chemistry on outer solar system bodies: Carboxylic acids, nitriles, and urea detected in refractory residues produced from the UV Photolysis of N_2:CH_4:Co-containing ices. *Astrophys. J.* **788**, 111 (2014).
37. C. K. Materese, D. P. Cruikshank, S. A. Sandford, H. Imanaka, M. Nuevo, Ice chemistry on outer solar system bodies: Electron radiolysis of N_2-, CH_4-, and CO-containing ices. *Astrophys. J.* **812**, 150 (2015).
38. H. Imanaka, B. N. Khare, J. E. Elsila, E. L. O. Bakes, C. P. McKay, D. P. Cruikshank, S. Sugita, T. Matsui, R. N. Zare. Laboratory experiments of Titan tholin formed in cold plasma at various pressures: Implications for nitrogen-containing polycyclic aromatic compounds in Titan haze. *Icarus* **168**, 344–366 (2004).
39. Y. Kebukawa, G. D. Cody, A kinetic study of the formation of organic solids from formaldehyde: Implications for the origin of extraterrestrial organic solids in primitive Solar System objects. *Icarus* **248**, 412–423 (2015).
40. M. Manga, C.-Y. Wang, Pressurized oceans and the eruption of liquid water on Europa and Enceladus. *Geophys. Res. Lett.* **34**, L07202 (2007).
41. M. Neveu, S. J. Desch, E. L. Shock, C. R. Glein, Prerequisites for explosive cryovolcanism on dwarf planet-class Kuiper belt objects. *Icarus* **246**, 48–64 (2015).
42. T. Caliński, J. Harabasz, A dendrite method for cluster analysis. *Commun. Stat.* **3**, 1–27 (1974).
43. G. Sill, U. Fink, J. R. Ferraro, Absorption coefficients of solid NH_3 from 50 to 7000 cm^{-1}. *J. Opt. Soc. Am.* **70**, 724–730 (1980).
44. U. Fink, G. T. Sill, The infrared spectral properties of frozen volatiles, in *Comets*, L. L. Wilkening, Ed. (University of Arizona Press, 1982), pp. 164–202.

45. R. M. E. Mastrapa, M. P. Bernstein, S. A. Sandford, T. L. Roush, D. P. Cruikshank, C. M. Dalle Ore, Optical constants of amorphous and crystalline H_2O-ice in the near infrared from 1.1 to 2.6 μm. *Icarus* **197**, 307–320 (2008).
46. B. Hapke, *Theory of Reflectance and Emittance (Topics in Remote Sensing)* (Cambridge Univ. Press, 1993).
47. Y. Shkuratov, L. Starukhina, H. Hoffmann, A. Gabriel, A model of spectral albedo of particulate surfaces: Implications for optical properties of the Moon. *Icarus* **137**, 235–246 (1999).

Acknowledgments
Funding: D.P.C., S.P., C.M.D.O., and other New Horizons team members acknowledge support from NASA's New Horizons Project. S.P, also gratefully acknowledges NASA grant no. NNX16AC83G for partial funding that supported this work. B.S. acknowledges the Centre National d'Etudes Spatiales (CNES) for its financial support through its "Système Solaire" program. **Author contributions:** C.M.D.O. and D.P.C.: data processing and evaluation; S.P., F.S., B.S., and J.C.C.: modeling of spectra; W.B.M., O.M.U., K.N.S., J.M.M., J.C.C., A.H.P., and S.A.S.: interpretation of geological setting; W.M.G., A.V., and C.B.O.: preparation of the initial LEISA datasets and interpretation of the spectra; H.A.W., L.A.Y., and K.E.: critical to New Horizons operations before and during spacecraft encounter with Pluto. All members of the New Horizons Surface Composition Science Theme Team contributed to the overall planning and execution of the mission and to the acquisition and processing of the data, and laid the foundation for understanding of Pluto's composition and geology upon which the results present here are based. **Competing interests:** The authors declare that they have no competing interests. **Data and materials availability:** All data needed to evaluate the conclusions in the paper are present in the paper. New Horizons spacecraft data are deposited in the NASA Planetary Data System (PDS) without restrictions. Additional data related to this paper may be requested from the authors.

Submitted 28 September 2018
Accepted 25 April 2019
Published 29 May 2019
10.1126/sciadv.aav5731

Citation: C. M. Dalle Ore, D. P. Cruikshank, S. Protopapa, F. Scipioni, W. B. McKinnon, J. C. Cook, W. M. Grundy, B. Schmitt, S. A. Stern, J. M. Moore, A. Verbiscer, A. H. Parker, K. N. Singer, O. M. Umurhan, H. A. Weaver, C. B. Olkin, L. A. Young, K. Ennico, New Horizons Surface Composition Science Theme Team, Detection of ammonia on Pluto's surface in a region of geologically recent tectonism. *Sci. Adv.* **5**, eaav5731 (2019).